High Redshift GRBs

Neil Gehrels* and John K. Cannizzo†

*Astroparticle Physics Division, NASA/Goddard Space Flight Center, Greenbelt, MD 20771, USA
†CRESST/Joint Center for Astrophysics, Univ. of Maryland, Baltimore County, Baltimore, MD 21250, USA

Abstract. The *Swift* mission has opened a new, high redshift window on the universe. In this review we provide an overview of gamma-ray burst (GRB) science, describe the *Swift* mission, discuss high−z GRBs and tools for high−z studies, and look forward at future capabilities. A new mission concept − *Lobster* − is described that would monitor the X-ray sky at order of magnitude higher sensitivity than current missions.

Keywords: Gamma rays: general - telescopes - bursts
PACS: 95.55.Ka, 95.85.Nv, 95.85.Pw, 97.60.Bw, 97.60.Lf, 98.62.Nx, 98.70.Rz

INTRODUCTION

GRBs are the most luminous explosions in the universe and are thought to be the birth cries of black holes. They are a product of the space age, discovered [29] by *Vela* and observed by satellites for 40 years. Despite impressive advances over the past three decades, the study of bursts remains highly dependent on the capabilities of the observatories carrying out the measurements. The era of the *Compton Gamma Ray Observatory (CGRO)* led to the discovery of more than 2600 bursts in just 9 years. Analyses of these data produced the key result that GRBs area isotropic on the sky and occur at a frequency of roughly two per day all sky [36]. The hint from earlier instruments was confirmed that GRBs come in two distinct classes of short and long bursts, with distributions crossing at ~ 2 s duration [30]. The *BeppoSAX* mission made the critical discovery of X-ray afterglows of long bursts [11]. With the accompanying discoveries by ground-based telescopes of optical [52] and radio [17] afterglows, long GRBs were found to emanate from star forming regions in host galaxies at a typical distance $z \simeq 1$. *BeppoSAX* and the following *HETE-2* mission also found evidence of associations of GRBs with Type Ic supernovae (SNe). This supported the growing evidence that long GRBs are caused by "collapsars" where the central core of a massive star collapses to a black hole [32].

The next chapter in our understanding of GRBs is being written by the *Swift* mission[19]. In this paper we discuss the findings of *Swift* and their relevance to our understanding of GRBs. We also examine what is being learned about star formation, SNe, and the early universe from the new results.

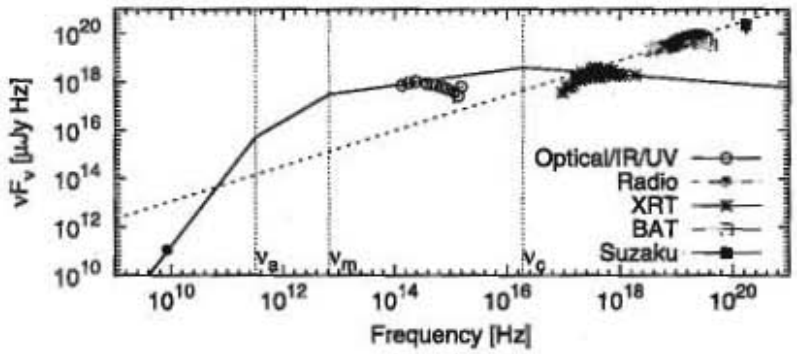

FIGURE 1. Broadband spectrum of GRB 051111 from radio to gamma-ray energies [10]. The dashed line, including the *Swift*/BAT and *Suzaku*/WAM data, indicates prompt emission. The solid line segments indicate a synchrotron fit to the afterglow emission, consisting of radio, optical, IR, UV, and X-ray data at $t = 100$s. The fit assumes an external shock expanding into a uniform-density medium, emitting synchrotron radiation. It is assumed that electrons are distributed as a power law in Lorentz factor γ above a minimum value γ_m according to $N(\gamma_e) \propto \gamma_e^{-p}$, for $\gamma_e > \gamma_m$. For $\nu < \nu_a$, the self-absorption frequency, the spectrum drops off steeply (ν^2). For $\nu_a < \nu < \nu_m$, the spectrum varies as $\nu^{1/3}$. The higher energy electrons cool first, hence one expects a time-dependent cooling frequency ν_c which decreases with time as $t^{-1/2}$. For $\nu_m < \nu < \nu_c$, the spectrum varies as $\nu^{-(p-1)/2}$, while for $\nu > \nu_c$, it varies as $\nu^{-p/2}$.

SWIFT GRBS

Swift [19] is a dedicated GRB observatory that is now measuring many properties of the prompt and afterglow radiation. It carries a wide-field Burst Alert Telescope (BAT) [2] that detects GRBs and positions them to arcmin accuracy, and the narrow-field X-Ray Telescope (XRT) [8] and UV-Optical Telescope (UVOT) [43] that observe their afterglows and determine positions to arcsec accuracy, all within ~100 s. The BAT detects the bursts in the $15 - 150$ keV band and determines a few-arc-min position onboard within 12 s. The position is provided to the spacecraft which is then re-pointed to the burst location in less than 2 minutes to allow XRT and UVOT observations of the afterglow.

As of 1 June 2012, BAT has detected 678 GRBs. Approximately 90% of the BAT-detected GRBs have repointings within 5 minutes (the remaining 10% have spacecraft constraints that prevent rapid slewing). Of those, virtually all bursts observed promptly have detected X-ray afterglow. Already, 80% of the known X-ray afterglows are from *Swift*. The fraction of rapid-pointing GRBs that have UVOT detection is ~30%. Combined with ground-based optical observations, about 60% of *Swift* GRBs have optical afterglow detection. Figure 1 shows a broadband GRB spectrum spanning more than ten decades in frequency.

GRBs come in two kinds, long and short, where the dividing line between the two is ~2 s [30]. A further division can be made spectrally according to their hardness ratio (i.e., ratio of high to low energies). The redshift range is from about 0.2 to 2 for short GRBs (sGRBs), with a mean of about 0.4. For long GRBs (lGRBs) the range is between about 0.009 and 9.4, with a mean of about 2.3. The typical energy release is $\sim 10^{49} - 10^{50}$ erg for sGRBs and $\sim 10^{50} - 10^{51.5}$ erg for lGRBs. These ranges are

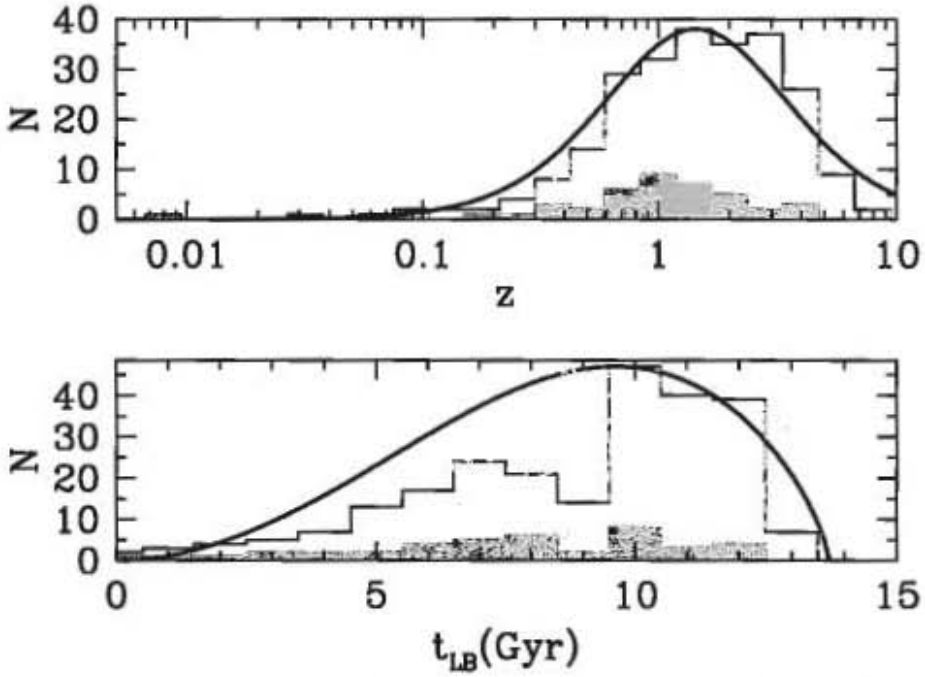

FIGURE 2. The frequency histogram distribution for all spectroscopic GRB redshifts determined to date (243 - shown in blue) as well as the pre-*Swift* era distribution (41 - shown in green). The top panel shows the distribution in z, and the bottom panel in look-back time. The red curves indicate the evolution of a slice of comoving volume $(dV/dz)(1+z)^{-1}$, where the factor $(1+z)^{-1}$ corrects for cosmological time dilation, given that the GRB rate has effect units of volume^{-1} time^{-1}.

based on observed isotropic-equivalent energies of $\sim 10^{51}$ erg for sGRBs and $\sim 10^{53}$ erg for lGRBs, and estimates for jet beaming for each class, $\theta_j \sim 5°$ for lGRBs and $\theta_j \sim 5-15°$ for sGRBs [9, 22, 15]. Beaming angles for sGRBs are still highly uncertain. The corresponding beaming factors $f_b = 1-\cos\theta_j \simeq \theta_j^2/2$ are roughly $1/300$ for lGRBs and $1/300 - 1/30$ for sGRBs. The $L_X/E_{\gamma-iso}$ values are similar between lGRBs and sGRBs. The sGRBs have weaker X-ray afterglows, a mean value of $\sim 7\times 10^{-10}$ erg cm^{-2} s^{-1} versus $\sim 3\times 10^{-9}$ erg cm^{-2} s^{-1} for lGRBs. Indirect arguments lead to inferred bulk Lorentz factors for the GRB jets of $\sim 10^2 - 10^3$.

HIGH REDSHIFT GRBS

Swift has brought about a revolution in GRB research. Redshifts from GRBs discovered prior to *Swift* amount to 41 total. (At the time of *Swift*'s launch this number was ~25, but continued observation of identified host galaxies with time has increased the pre-*Swift* total.) Now there are over 200 redshifts. Figure 2 shows a plot of frequency histogram distribution for redshifts, excluding uncertain values and photometric redshifts. As a first approximation, the GRB rate history traces the volume of the universe, as shown by the red curves in Figure 2. Of the 243 total redshifts we have now, 187 are from GRBs

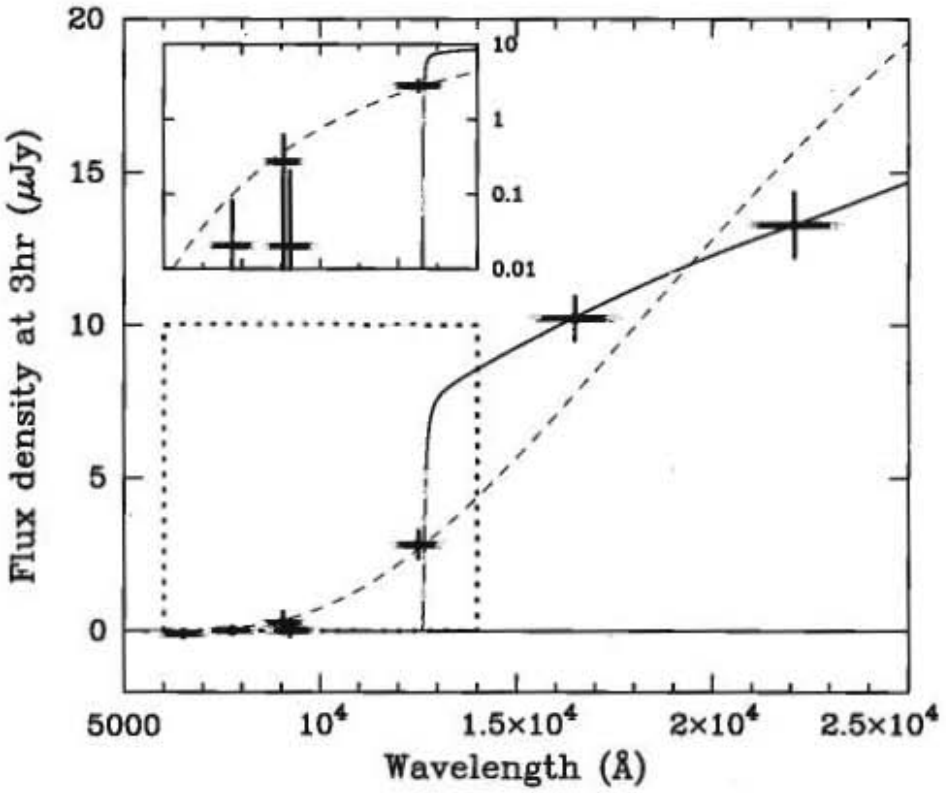

FIGURE 3. Spectrum of the highest redshift GRB to date, GRB090429B, with an indicated photometric redshift of ~9.4 ([12]). The cosmological shift in wavelength $1+z$ of the 91.2 nm rest frame Lyman edge is more than a factor of 10.

discovered by *Swift*. There are 18 from *HETE-2*, 15 from *BeppoSax*, 10 from *IPN*, 6 from *Fermi*, and 4 from *INTEGRAL*.

Swift is detecting GRBs at higher redshift than previous missions due to its higher sensitivity and rapid afterglow observations. The average redshift for the *Swift* GRBs is 2.3 compared to 1.2 for previous observations. Although statistics are poor, the highest redshift GRBs are seen to have high luminosity, resulting in fluxes well above the detection threshold. Such bursts are also strong at other wavelengths. Table 1 presents optical data for the highest redshift GRBs observed to date, where the look-back time t_{LB}(Gyr) is given in the second column.

To date, *Swift* has seen seven GRBs with $z > 5$. The highest z GRBs so far are $z = 6.3$ (GRB 050904 −[27]), $z = 6.7$ (GRB 080913 − [21]), $z = 8.2$ (GRB 090423 − [44, 49]), and $z = 9.4$ (GRB 090429B − [12]). Figure 3 shows a spectrum of the current record holder GRB 090429B [12]. Because GRBs are so bright across the electromagnetic spectrum, they are excellent tools for studying the high redshift universe. The information that can be provided by GRBs is complementary to what can be learned by studies of galaxies and quasars. For example, at $z > 8$ it is expected that the bulk of the star formation activity is taking place in small galaxies below the detection limits of *HST*, and even

TABLE 1. High z GRBs.

z	t_{LB}(Gyr)	GRB	Brightness		
9.4	13.1	090429B	$K = 19$	@	3 hr
8.2	13.0	090423	$K = 20$	@	20 min
6.7	12.8	080913	$K = 19$	@	10 min
6.3	12.8	050904	$J = 18$	@	3 hr
5.6	12.6	060927	$I = 16$	@	2 min
5.3	12.6	050814	$K = 18$	@	23 hr
5.11	12.5	060522	$R = 21$	@	1.5 hr

that expected for *JWST*, but their existence and properties may be inferred by studying the GRBs they produce. GRBs are superior probes of reionization to quasars because: (i) they do not modify their surroundings on large scales and hence probe the pristine IGM during reionization; and (ii) they lack intrinsic Lyα emission, which in the case of quasars masks the damping wing of the IGM neutral H and prevents an accurate measurement of the neutral fraction. Also, the massive star progenitors of GRBs predate the supermassive black holes that power luminous quasars.

By measuring absorption lines in the optical/IR spectrum, the elemental abundances can be determined. GRBs can thereby be used to determine the metallicity of their host galaxy to high redshift [46, 47]. GRBs are also being used to determine the star formation rate to high redshift [28, 42, 51]. Figure 4 shows an example of data points on the star formation plot from GRBs. Corrections need to be made for systematic effects that alter the proportionality between measured GRB rates and inferred star formation rates, such as possible metallicity bias.

SHORT GRBS

At *Swift*'s launch, the greatest mystery of GRB astronomy was the nature of short-duration, hard-spectrum bursts. Although more than 50 long GRBs had afterglow detections, no afterglow had been found for any short burst. In May 2005 (GRB 050509B), *Swift* provided the first short GRB X-ray afterglow localization [20]. This burst plus the *HETE-2* GRB 050709 and *Swift* GRB 050724 led to a breakthrough in our understanding [20, 5, 16, 53, 25, 3, 4] of short bursts. Since the launch of *Swift* there have been 66 sGRBs localized (there were none prior to *Swift*). Most of these have XRT detections, and about one third have host identifications or redshifts. Two of the localizations are from sGRBs detected by *HETE-2*, one by *INTEGRAL*, and one by *Fermi*/LAT.

In stark contrast to long bursts, the evidence to date on short bursts is that they can originate from regions with low star formation rate. GRB 050509B and 050724 were from elliptical galaxies with low current star formation rates while GRB 050709 was from a region of a star forming galaxy with no nebulosity or evidence of recent star formation activity in that location. Recent *HST* observations of locations of sGRBs in their hosts reveal that short bursts trace the light distribution of their hosts while long bursts are concentrated in the brightest regions [14]. sGRBs are also different from lGRBs in that accompanying SNe are not detected for nearby events [5, 16, 25]. Taken

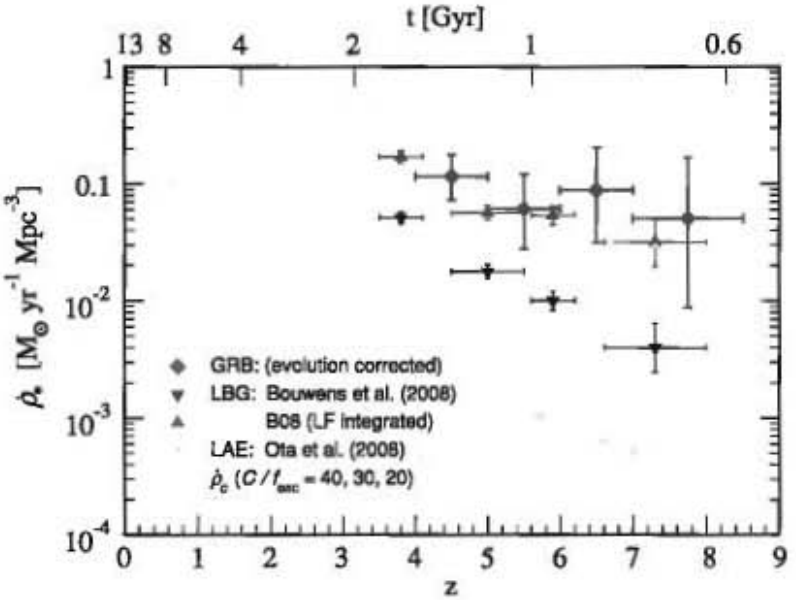

FIGURE 4. The cosmic star formation rate (SFR) history [28], with data from several sources [26, 7, 38]. The rates inferred from high−z GRBs are shown as diamonds. The three dashed curves [33] give the critical SFR $\dot{\rho}_c$ required to balance recombination, for $C/f_{esc} = 40$, 30, and 20 (top to bottom), where C is the clumpiness of the intergalactic medium and f_{esc} the fraction of photons that escape their galaxy.

together, these results support the interpretation that short bursts are associated with an old stellar population, and may arise from mergers of compact binaries [i.e., double neutron star or neutron star - black hole (NS-BH) binaries].

OPEN ISSUES

At the time of *Swift*'s launch, a basic paradigm had developed, which is now less certain than before. The concept of "achromatic breaks" in the decay light curves – or steepenings that occur simultaneously across many wavebands – had been predicted by theory [40, 41, 45], and was thought to have observational confirmation [18]. The expectation for *Swift* was that it would provide many more examples of such decays, thereby strengthening and enriching the underlying paradigm.

In fact, the opposite has proven to be true [37, 39, 31]. With much better data than before, we only see a small handful of achromatic breaks [6, 48, 13, 54]. A more critical look back at the pre-*Swift* examples shows that they were based on very fragmentary data. The "best" pre-*Swift* case, GRB 990510 [23], is based on data spanning only a factor $\sim$2 in wavelength, and therefore could be dominated by a single broadband feature in the spectrum.

Although we have made theoretical advances based on ab initio calculations of jet launching from Kerr black holes in recent years, the clues from observations have been ambiguous concerning the issue of whether the jet is Poynting flux dominated or matter

dominated. The theoretical calculations indicate the former [34, 24, 35, 50], but it would be good to have observational verification.

FUTURE DIRECTIONS – THE *LOBSTER* MISSION CONCEPT

The tantalizing glimpses of high$-z$ GRBs detected by *Swift* have underscored the desire to have a more powerful discovery mission tuned for the faint, red-shifted emission of distant events. To this end, *Lobster* is a mission concept led by Goddard Space Flight Center, MIT, the Univ. of Leicester, and the Univ. of Arizona that combines an X-ray wide field imager (WFI) with narrow field IR telescope (IRT). The underlying strategy is similar to that of *Swift*: first a detection at high energies, followed up by more detailed observations. The WFI has a combined 0.5 sr field of view that covers ~50% of the sky every 3 hr in multiple pointings. It is based on CCD technology and lobster-eye microchannel optics [1]. The IRT has a 40 cm diameter mirror, a wavelength range of $0.6-2.1\mu$, and is capable of multiband photometry and $\lambda/\delta\lambda = 30$ slit spectroscopy.

Lobster will provide capabilities for a major step forward in high redshift universe studies using GRBs. The prompt emission is detected by the WFIs and observed in X-ray afterglow by the WFIs and infrared afterglow by the IRT. Improvements over *Swift* include: (1) more sensitive wide-field instrument, (2) infrared band follow-up telescope, and (3) slit spectroscopy with the follow-up telescope. The mission is predicted to detect more than 25 bursts per year at redshift $z > 5$ and extend detections to $z > 12$.

SUMMARY

GRBs are the most luminous sources in the universe. The highest redshift long GRBs are easily detected, thus the long GRBs constitute the only volume-limited class of objects in astronomy for which the "volume" is the universe itself. Long GRBs have been detected to $z > 8$. Spectroscopy of optical afterglow allows us to determine the chemical composition and ionization state of the host galaxy and intervening line-of-sight material, as well as the star formation rate. Many high$-z$ GRB candidates do not have adequate immediate follow-up, and for some (such as the current record holder, GRB 090429B) the high redshifts are determined only after much follow-up work. The prospects are good for future improvements in understanding high$-z$ GRBs.

REFERENCES

1. Angel, J. R. P. 1979, *ApJ*, 233, 364
2. Barthelmy, S. D. et al. 2005a, *Sp Sci Rev*, 120, 175
3. Barthelmy, S. D., et al. 2005b, *Nature*, 438, 994
4. Berger, E., et al. 2005, *Nature*, 438, 988
5. Bloom, J. S., et al. 2006, *ApJ*, 638, 354
6. Blustin, A. J., et al. 2006, *ApJ*, 637, 901
7. Bouwens, R. J., et al. 2008, *ApJ*, 686, 230
8. Burrows, D. N., et al. 2005, *Sp Sci Rev*, 120, 165

9. Burrows, D. N., et al. 2006, *ApJ*, 653, 468
10. Butler, N. R., et al. 2006, *ApJ*, 652, 1390
11. Costa, E., et al. 1997, *Nature*, 387, 783
12. Cucchiara, A., et al. 2011, *ApJ*, 736, 7
13. Dai, X., Halpern, J. P., Morgan, N. D., Armstrong, E., Mirabal, N., Haislip, J. B., Reichart, D. E., & Stanek, K. Z. 2007, *ApJ*, 658, 509
14. Fong, W., Berger, E., & Fox, D. B. 2010, *ApJ*, 708, 9
15. Fong, W., et al. 2012, astro-ph/1204.5475
16. Fox, D. B., et al. 2005, *Nature*, 437, 845
17. Frail, D. A., Kulkarni, S. R., Nicastro, L., Feroci, M., & Taylor, G. B. 1997, *Nature*, 389, 261
18. Frail, D. A., et al. 2001, *ApJ*, 562, L55
19. Gehrels, N., et al. 2004, *ApJ*, 611, 1005
20. Gehrels, N., et al. 2005, *Nature*, 437, 851
21. Greiner, J., et al. 2009, *ApJ*, 693, 1610
22. Grupe, D., Burrows, D. N., Patel, S. K., Kouveliotou, C., Zhang, B., Mészáros, P., Wijers, R. A. M., & Gehrels, N. 2006, *ApJ*, 653, 462
23. Harrison, F. A., et al. 1999, *ApJ*, 523, L121
24. Hawley, J. F., & Krolik, J. H. 2006, *ApJ*, 641, 103
25. Hjorth, J., et al. 2005, *Nature*, 437, 859
26. Hopkins, A. M., & Beacom, J. F. 2006, *ApJ*, 651, 143
27. Kawai, N. et al. 2006, *Nature*, 440, 184
28. Kistler, M. D., Yüksel, H., Beacom, J. F., Hopkins, A. M., & Wyithe, J. S. B. 2009, *ApJ*, 705, L104
29. Klebesadel, R. W., Strong, I. B., & Olson, R. A. 1973, *ApJ*, 182, L85
30. Kouveliotou, C., Meegan, C. A., Fishman, G. J., Bhat, N. P., Briggs, M. S., Koshut, T. M., Paciesas, W. S., & Pendleton, G. N. 1993, *ApJ*, 413, L101
31. Liang, E.-W., Racusin, J. L., Zhang, B., Zhang, B.-B., & Burrows, D. N. 2008, *ApJ*, 675, 528
32. MacFadyen, A. I., & Woosley, S. E. 1999, *ApJ*, 524, 262
33. Madau, P., Haardt, F., & Rees, M. J. 1999, *ApJ*, 514, 648
34. McKinney, J. C. 2005, *ApJ*, 630, L5
35. McKinney, J. C., & Blandford, R. D. 2009, *MNRAS*, 394, L126
36. Meegan, C. A., Fishman, G. J., Wilson, R. B., Horack, J. M., Brock, M. N., Paciesas, W. S., Pendleton, G. N., & Kouveliotou, C. 1991, *Nature*, 355, 143
37. Oates, S. R., et al. 2007, *MNRAS*, 380, 270
38. Ota, K., et al. 2008, *ApJ*, 677, 12
39. Racusin, J. L., et al. 2008, *Nature*, 455, 183
40. Rhoads, J. E. 1997, *ApJ*, 487, L1
41. Rhoads, J. E. 1999, *ApJ*, 525, 737
42. Robertson, B. E., & Ellis, R. S. 2012, *ApJ*, 744, 95
43. Roming, P. W. A., et al. 2005, *Sp. Sci. Rev.*, 120, 95
44. Salvaterra, R., et al. 2009, *Nature*, 461, 1258
45. Sari, R., Piran, T., & Halpern, J. P. 1999, *ApJ*, 519, L17
46. Savaglio, S. 2006, *New J Phys*, 8, 195
47. Savaglio, S., et al. 2012, *MNRAS*, 420, 627
48. Stanek, K. Z., et al. 2007, *ApJ*, 654, L21
49. Tanvir, N. R., et al. 2009, *Nature*, 461, 1254
50. Tchekhovskoy, A., & McKinney, J. C. 2012, *MNRAS*, 423, L55
51. Trenti, M., Perna, R., Levesque, E. M., Shull, J. M., & Stocke, J. T. 2012, *ApJ*, 749, L38
52. van Paradijs, J., et al. 1997, *Nature*, 386, 686
53. Villasenor, J. S., et al. 2005, *Nature*, 437, 855
54. Willingale, R., et al. 2007, *ApJ*, 662, 1093